

Studies of the Decay $B^\pm \rightarrow D_{CP}K^\pm$

K. Abe,⁸ K. Abe,⁴³ N. Abe,⁴⁶ R. Abe,²⁹ T. Abe,⁴⁴ Byoung Sup Ahn,¹⁵ H. Aihara,⁴⁵ M. Akatsu,²² Y. Asano,⁵⁰ T. Aso,⁴⁹ V. Aulchenko,² T. Aushev,¹² A. M. Bakich,⁴⁰ Y. Ban,³³ P. K. Behera,⁵¹ I. Bizjak,¹³ A. Bondar,² A. Bozek,²⁷ M. Bračko,^{20,13} T. E. Browder,⁷ B. C. K. Casey,²⁶ M.-C. Chang,²⁶ P. Chang,²⁶ Y. Chao,³⁹ B. G. Cheon,¹² R. Chistov,³⁹ Y. Choi,³⁹ Y. K. Choi,³⁹ M. Danilov,¹² L. Y. Dong,¹⁰ A. Drutskoy,¹² S. Eidelman,² V. Eiges,¹² Y. Enari,²² F. Fang,⁷ H. Fujii,⁸ C. Fukunaga,⁴⁷ N. Gabyshev,⁸ A. Garmash,^{2,8} T. Gershon,⁸ B. Golob,^{19,13} A. Gordon,²¹ R. Guo,²⁴ J. Haba,⁸ T. Hara,³¹ Y. Harada,²⁹ H. Hayashii,²³ M. Hazumi,⁸ E. M. Heenan,²¹ I. Higuchi,⁴⁴ T. Higuchi,⁴⁵ L. Hinz,¹⁸ T. Hokuue,²² Y. Hoshi,⁴³ S. R. Hou,²⁶ W.-S. Hou,²⁶ S.-C. Hsu,²⁶ H.-C. Huang,²⁶ T. Igaki,²² Y. Igarashi,⁸ T. Iijima,²² K. Inami,²² A. Ishikawa,²² H. Ishino,⁴⁶ R. Itoh,⁸ H. Iwasaki,⁸ Y. Iwasaki,⁸ H. K. Jang,³⁸ J. H. Kang,⁵⁴ J. S. Kang,¹⁵ N. Katayama,⁸ Y. Kawakami,²² N. Kawamura,¹ T. Kawasaki,²⁹ H. Kichimi,⁸ D. W. Kim,³⁹ Heejong Kim,⁵⁴ H. J. Kim,⁵⁴ H. O. Kim,³⁹ Hyunwoo Kim,¹⁵ S. K. Kim,³⁸ T. H. Kim,⁵⁴ K. Kinoshita,⁵ S. Korpar,^{20,13} P. Križan,^{19,13} P. Krokovny,² R. Kulasiri,⁵ S. Kumar,³² A. Kuzmin,² Y.-J. Kwon,⁵⁴ J. S. Lange,^{6,35} G. Leder,¹¹ S. H. Lee,³⁸ J. Li,³⁷ A. Limosani,²¹ D. Liventsev,¹² R.-S. Lu,²⁶ J. MacNaughton,¹¹ G. Majumder,⁴¹ F. Mandl,¹¹ D. Marlow,³⁴ T. Matsuishi,²² S. Matsumoto,⁴ T. Matsumoto,⁴⁷ W. Mitaroff,¹¹ K. Miyabayashi,²³ Y. Miyabayashi,²² H. Miyake,³¹ H. Miyata,²⁹ G. R. Moloney,²¹ T. Mori,⁴ A. Murakami,³⁶ T. Nagamine,⁴⁴ Y. Nagasaka,⁹ T. Nakadaira,⁴⁵ E. Nakano,³⁰ M. Nakao,⁸ J. W. Nam,³⁹ Z. Natkaniec,²⁷ K. Neichi,⁴³ S. Nishida,¹⁶ O. Nitoh,⁴⁸ S. Noguchi,²³ T. Nozaki,⁸ S. Ogawa,⁴² T. Ohshima,²² T. Okabe,²² S. Okuno,¹⁴ S. L. Olsen,⁷ Y. Onuki,²⁹ W. Ostrowicz,²⁷ H. Ozaki,⁸ P. Pakhlov,¹² H. Palka,² C. W. Park,¹⁵ H. Park,¹⁷ L. S. Peak,⁴⁰ J.-P. Perroud,¹⁸ M. Peters,⁷ L. E. Piiilonen,⁵² J. L. Rodriguez,⁷ F. J. Ronga,¹⁸ N. Root,² M. Rozanska,²⁷ K. Rybicki,²⁷ H. Sagawa,⁸ S. Saitoh,⁸ Y. Sakai,⁸ M. Satpathy,⁵¹ A. Satpathy,^{8,5} O. Schneider,¹⁸ S. Schrenk,⁵ C. Schwanda,^{8,11} S. Semenov,¹² K. Senyo,²² R. Seuster,⁷ M. E. Sevier,²¹ H. Shibuya,⁴² B. Shwartz,² V. Sidorov,² J. B. Singh,³² S. Stanič,^{50,*} M. Starič,¹³ A. Sugi,²² A. Sugiyama,²² K. Sumisawa,⁸ T. Sumiyoshi,⁴⁷ K. Suzuki,⁸ S. Suzuki,⁵³ S. Y. Suzuki,⁸ S. K. Swain,⁷ T. Takahashi,³⁰ F. Takasaki,⁸ K. Tamai,⁸ N. Tamura,²⁹ J. Tanaka,⁴⁵ M. Tanaka,⁸ G. N. Taylor,²¹ Y. Teramoto,³⁰ S. Tokuda,²² S. N. Tovey,²¹ K. Trabelsi,⁷ T. Tsuboyama,⁸ T. Tsukamoto,⁸ S. Uehara,⁸ K. Ueno,²⁶ Y. Unno,³ S. Uno,⁸ Y. Ushiroda,⁸ G. Varner,⁷ K. E. Varvell,⁴⁰ C. C. Wang,²⁶ C. H. Wang,²⁵ J. G. Wang,⁵² M.-Z. Wang,²⁶ Y. Watanabe,⁴⁶ E. Won,¹⁵ B. D. Yabsley,⁵² Y. Yamada,⁸ A. Yamaguchi,⁴⁴ Y. Yamashita,²⁸ M. Yamauchi,⁸ H. Yanai,²⁹ P. Yeh,²⁶ Y. Yuan,¹⁰ Y. Yusa,⁴⁴ J. Zhang,⁵⁰ Z. P. Zhang,³⁷ Y. Zheng,⁷ V. Zhilich,² and D. Žontar⁵⁰

(The Belle Collaboration)

¹Aomori University, Aomori

²Budker Institute of Nuclear Physics, Novosibirsk

³Chiba University, Chiba

⁴Chuo University, Tokyo

⁵University of Cincinnati, Cincinnati Ohio

⁶University of Frankfurt, Frankfurt

⁷University of Hawaii, Honolulu Hawaii

⁸High Energy Accelerator Research Organization (KEK), Tsukuba

⁹Hiroshima Institute of Technology, Hiroshima

¹⁰Institute of High Energy Physics, Chinese Academy of Sciences, Beijing

¹¹Institute of High Energy Physics, Vienna

¹²Institute for Theoretical and Experimental Physics, Moscow

¹³J. Stefan Institute, Ljubljana

¹⁴Kanagawa University, Yokohama

¹⁵Korea University, Seoul

¹⁶Kyoto University, Kyoto

¹⁷Kyungpook National University, Taegu

¹⁸Institut de Physique des Hautes Énergies, Université de Lausanne, Lausanne

¹⁹University of Ljubljana, Ljubljana

²⁰University of Maribor, Maribor

²¹University of Melbourne, Victoria

²²Nagoya University, Nagoya

²³Nara Women's University, Nara

²⁴National Kaohsiung Normal University, Kaohsiung

²⁵National Lien-Ho Institute of Technology, Miao Li

- ²⁶National Taiwan University, Taipei
²⁷H. Niewodniczanski Institute of Nuclear Physics, Krakow
²⁸Nihon Dental College, Niigata
²⁹Niigata University, Niigata
³⁰Osaka City University, Osaka
³¹Osaka University, Osaka
³²Panjab University, Chandigarh
³³Peking University, Beijing
³⁴Princeton University, Princeton New Jersey
³⁵RIKEN BNL Research Center, Brookhaven New York
³⁶Saga University, Saga
³⁷University of Science and Technology of China, Hefei
³⁸Seoul National University, Seoul
³⁹Sungkyunkwan University, Suwon
⁴⁰University of Sydney, Sydney New South Wales
⁴¹Tata Institute of Fundamental Research, Bombay
⁴²Toho University, Funabashi
⁴³Tohoku Gakuin University, Tagajo
⁴⁴Tohoku University, Sendai
⁴⁵University of Tokyo, Tokyo
⁴⁶Tokyo Institute of Technology, Tokyo
⁴⁷Tokyo Metropolitan University, Tokyo
⁴⁸Tokyo University of Agriculture and Technology, Tokyo
⁴⁹Toyama National College of Maritime Technology, Toyama
⁵⁰University of Tsukuba, Tsukuba
⁵¹Utkal University, Bhubaneswer
⁵²Virginia Polytechnic Institute and State University, Blacksburg, Virginia
⁵³Yokkaichi University, Yokkaichi
⁵⁴Yonsei University, Seoul

(Received 2 July 2002; published 3 April 2003)

We report studies of the Cabibbo-suppressed decay $B^\pm \rightarrow D_{CP}K^\pm$, where D_{CP} denotes CP eigenstates of the $D^0 - \bar{D}^0$ system. The analysis is based on a 29.1 fb^{-1} sample collected at the $\Upsilon(4S)$ resonance with the Belle detector at the KEKB asymmetric e^+e^- storage ring. We measure ratios of branching fractions, relative to Cabibbo-favored $B^\pm \rightarrow D_{CP}\pi^\pm$, of $\mathcal{B}(B^- \rightarrow D_1K^-)/\mathcal{B}(B^- \rightarrow D_1\pi^-) = 0.125 \pm 0.036 \pm 0.010$ and $\mathcal{B}(B^- \rightarrow D_2K^-)/\mathcal{B}(B^- \rightarrow D_2\pi^-) = 0.119 \pm 0.028 \pm 0.006$; the index 1 (2) denotes the $CP = +1$ (-1) eigenstate. We also extract the partial rate asymmetries for $B^\pm \rightarrow D_{CP}K^\pm$, finding $\mathcal{A}_1 = 0.29 \pm 0.26 \pm 0.05$ and $\mathcal{A}_2 = -0.22 \pm 0.24 \pm 0.04$.

DOI: 10.1103/PhysRevLett.90.131803

PACS numbers: 13.25.Hw, 11.30.Er, 12.15.Hh

Direct CP violation in $B^\pm \rightarrow D_{CP}K^\pm$ decay, where D_{CP} denotes neutral D mesons that decay to CP eigenstates, provides a promising way to extract the angle ϕ_3 of the Cabibbo-Kobayashi-Maskawa (CKM) unitarity triangle [1,2]. A partial rate asymmetry \mathcal{A}_{CP} between the $D_{CP}K^-$ and $D_{CP}K^+$ final states can arise from interference between $b \rightarrow c$ and $b \rightarrow u$ processes. The relation of \mathcal{A}_{CP} and the ϕ_3 angle [3] is given by

$$\begin{aligned} \mathcal{A}_{1,2} &\equiv \frac{\mathcal{B}(B^- \rightarrow D_{1,2}K^-) - \mathcal{B}(B^+ \rightarrow D_{1,2}K^+)}{\mathcal{B}(B^- \rightarrow D_{1,2}K^-) + \mathcal{B}(B^+ \rightarrow D_{1,2}K^+)} \\ &= \frac{2r \sin \delta' \sin \phi_3}{1 + r^2 + 2r \cos \delta' \cos \phi_3}, \end{aligned} \quad (1)$$

where indices 1 and 2 denote the $CP = +1$ and $CP = -1$ eigenstates of the neutral D mesons, r is the ratio of the amplitudes, $r \equiv |A(B^- \rightarrow \bar{D}^0K^-)/A(B^- \rightarrow D^0K^-)|$, and δ' is the strong phase difference between the two ampli-

tudes, with $\delta' = \delta$ for D_1 and $\delta' = \delta + \pi$ for D_2 . This asymmetry can have a nonzero value when both ϕ_3 and δ are nonzero. In principle, one can constrain the angle ϕ_3 from the measurement of asymmetries $\mathcal{A}_{1,2}$.

$B \rightarrow DK$ processes have been studied by measuring the ratio of the Cabibbo-suppressed process $B^- \rightarrow D^0K^-$ to the Cabibbo-favored process $B^- \rightarrow D^0\pi^-$. Belle [4] measured $R = \mathcal{B}(B^- \rightarrow D^0K^-)/\mathcal{B}(B^- \rightarrow D^0\pi^-) = 0.079 \pm 0.009 \pm 0.006$, while CLEO [5] reported $R = 0.055 \pm 0.014 \pm 0.005$. Both measurements are in agreement with the naïve theoretical expectation: assuming factorization, $R = \tan^2 \theta_C (f_K/f_\pi)^2 \approx 0.074$ in a tree-level approximation, where θ_C is the Cabibbo angle, and f_K and f_π are the decay constants.

In this Letter, we report the first measurement of $B^\pm \rightarrow D_{CP}K^\pm$ decay. We also give a comparison of the ratio of branching fractions R for the flavor specific state and the $CP = \pm 1$ eigenstates, and a determination of the

asymmetries $\mathcal{A}_{1,2}$. The results are based on a 29.1 fb^{-1} data sample collected on the $Y(4S)$ resonance with the Belle detector [6] at the KEKB asymmetric e^+e^- collider [7], corresponding to approximately $31.3 \times 10^6 B\bar{B}$ events. The inclusion of charge conjugate decay modes is implied throughout this Letter unless otherwise stated.

Belle is a general-purpose detector with a 1.5 T superconducting solenoid magnet that can distinguish the Cabibbo-suppressed (-favored) processes $B^- \rightarrow D^0 K^-$ ($D^0 \pi^-$) by means of particle identification and kinematic separation. A detailed description of the Belle detector can be found elsewhere [6].

We distinguish the processes $B^- \rightarrow D^0 h^-$, $h^- = K^-, \pi^-$, using particle identification of the prompt hadron h^- and the effect of the mass difference at the final stage of event selection. The decay $B^- \rightarrow D^0 \pi^-$ is used as a control sample to establish constraints on kinematic variables, resolution of detectors, evaluation of systematic uncertainties, and normalization of results.

Flavor specific D^0 meson candidates (denoted D_f) are reconstructed via $D^0 \rightarrow K^- \pi^+$; for $CP = +1$ eigenstates we use $D_1 \rightarrow K^- K^+$ and $\pi^- \pi^+$ and for $CP = -1$ we use $D_2 \rightarrow K_S \pi^0$, $K_S \omega$, $K_S \phi$, $K_S \eta$, and $K_S \eta'$.

$K_S \rightarrow \pi^+ \pi^-$ candidates are reconstructed from oppositely charged tracks with an invariant mass within $\pm 3\sigma$ of the nominal K_S mass. We impose a photon energy cut $E_\gamma > 30 \text{ MeV}$ to reconstruct $\pi^0 \rightarrow \gamma\gamma$, and require an invariant mass within $\pm 3\sigma$ of the nominal value. $\eta \rightarrow \gamma\gamma$ and $\eta' \rightarrow \eta \pi^+ \pi^-$ candidates are reconstructed using mass cuts $0.495 \text{ GeV}/c^2 < M(\gamma\gamma) < 0.57 \text{ GeV}/c^2$ and $0.904 \text{ GeV}/c^2 < M(\eta \pi^+ \pi^-) < 1.003 \text{ GeV}/c^2$, and a momentum cut $p_\eta > 500 \text{ MeV}/c$.

Vector meson decays $\omega \rightarrow \pi^+ \pi^- \pi^0$ and $\phi \rightarrow K^+ K^-$ are reconstructed requiring $0.733 \text{ GeV}/c^2 < M(\pi^+ \pi^- \pi^0) < 0.819 \text{ GeV}/c^2$ and $1.007 \text{ GeV}/c^2 < M(K^+ K^-) < 1.031 \text{ GeV}/c^2$; a helicity angle cut $|\cos\theta_{\text{hel}}| > 0.4$ reduces the nonresonant $D^0 \rightarrow K_S \pi^+ \pi^- \pi^0$ and $K_S K^+ K^-$ backgrounds to a negligible level [8]. For $D^0 \rightarrow K_S \omega$, the $D^0 \rightarrow K^{*-} \rho^+$ background is rejected by vetoing $K_S \pi^-$ combinations within $\pm 75 \text{ MeV}/c^2$ of the nominal K^* mass.

For each charged track, the particle identification system is used to determine likelihoods \mathcal{L}_K , \mathcal{L}_π , and the K/π likelihood ratio $P(K/\pi) = \mathcal{L}_K/(\mathcal{L}_K + \mathcal{L}_\pi)$ [6]. We identify pions using $P(K/\pi) < 0.7$ for $D^0 \rightarrow K^- \pi^+$ and $\pi^- \pi^+$; kaons are required to satisfy $P(K/\pi) > 0.3$ for $D^0 \rightarrow K^- \pi^+$ and $P(K/\pi) > 0.7$ for $D^0 \rightarrow K^- K^+$. Pions from $D^0 \rightarrow \pi^- \pi^+$ are required to have momentum $p > 0.8 \text{ GeV}/c$, and the D^0 candidate is vetoed if either pion, when combined with any other track in the event, has an invariant mass within $\pm 50 \text{ MeV}/c^2$ of the nominal J/ψ mass, or $\pm 20 \text{ MeV}/c^2$ of the nominal D^0 mass.

Candidate D^0 mesons are also required to have an invariant mass within $\pm 2.5\sigma$ of the nominal value, where σ is the measured mass resolution, which ranges from 5 to $18 \text{ MeV}/c^2$, depending on the decay channel.

To improve the momentum determination, tracks and photons from the D^0 candidate final states, except for $K_S \pi^0$, $K_S \eta$, and $K_S \eta'$, are then refitted according to the nominal D^0 mass hypothesis and the reconstructed vertex position.

We analyze $B^- \rightarrow DK^-$ and $D\pi^-$ events using the variables ΔE and M_{lc} . The energy difference in the center of mass frame (c.m.) is calculated by assigning the pion mass to the prompt hadron h^- : $\Delta E = E_D^{\text{c.m.}} + E_h^{\text{c.m.}} - E_{\text{beam}}^{\text{c.m.}}$. The laboratory constrained mass is the B candidate mass calculated from laboratory momenta, assuming $e^+e^- \rightarrow B\bar{B}$: $M_{lc} = \sqrt{(E_B^{\text{lab}})^2 - (p_B)^2}$, where $E_B^{\text{lab}} = \frac{1}{E_{ee}}(s/2 + \mathbf{p}_{ee} \cdot \mathbf{p}_B)$, \mathbf{p}_B is the laboratory momentum of the B meson candidate ($p_B = |\mathbf{p}_B|$), \mathbf{p}_{ee} and E_{ee} are the laboratory momentum and energy of the e^+e^- system, and s is the square of the c.m. energy. We accept B candidates with $5.27 \text{ GeV}/c^2 < M_{lc} < 5.29 \text{ GeV}/c^2$.

Background events from $e^+e^- \rightarrow q\bar{q}$ continuum processes are rejected using event shape variables that distinguish between spherical $B\bar{B}$ events and jetlike continuum events. We construct a Fisher discriminant, $\mathcal{F} = \sum_{l=2,4} \alpha_l R_l^{s0} + \sum_{l=1} \beta_l R_l^{o0}$, where α_l , β_l are coefficients maximizing discrimination between $B\bar{B}$ and continuum events, and R_l^{s0} , R_l^{o0} are modified Fox-Wolfram moments [9]. We also use the angle θ_B between the beam axis and the c.m. momentum of the B meson. A likelihood variable is formed from the probability density functions of \mathcal{F} and $\cos\theta_B$, for the signal (\mathcal{L}_{sig}) and the continuum background ($\mathcal{L}_{\text{cont}}$); we then apply cuts on the likelihood ratio $\mathcal{LR} = \mathcal{L}_{\text{sig}}/(\mathcal{L}_{\text{sig}} + \mathcal{L}_{\text{cont}})$. Since each D^0 decay mode has different backgrounds, we optimize the \mathcal{LR} cut for each mode by maximizing $S/\sqrt{S+N}$, where S (N) denotes the number of signal (background) events estimated by a Monte Carlo simulation [10]. For example, for the $D^0 \rightarrow K^- \pi^+$ mode, we require $\mathcal{LR} > 0.4$, retaining 87.1% of signal and 26.4% of the continuum background.

We use particle identification information on the prompt hadron to divide the remaining events into samples enriched in $B^- \rightarrow D^0 K^-$ [$P(K/\pi) > 0.8$], and $B^- \rightarrow D^0 \pi^-$ [$P(K/\pi) < 0.8$]. The ΔE distribution is then used to distinguish between $B^- \rightarrow D^0 K^-$ (peaking at -49 MeV) and $B^- \rightarrow D^0 \pi^-$ (peaking at 0 MeV), as shown in Fig. 1. In the $B^- \rightarrow D^0 K^-$ enriched sample a second peak near $\Delta E = 0 \text{ MeV}$, due to misidentified pions from $B^- \rightarrow D^0 \pi^-$, can be seen in Figs. 1(b), 1(d), and 1(f).

The numbers of $B^- \rightarrow D^0 \pi^-$ and $B^- \rightarrow D^0 K^-$ events are extracted by fitting double Gaussian functions with different central values and widths to the ΔE distribution. Backgrounds originate from $q\bar{q}$ continuum events and $B\bar{B}$ events. Continuum events are distributed over the entire ΔE region, and the shape of this background is determined by fitting a linear function to

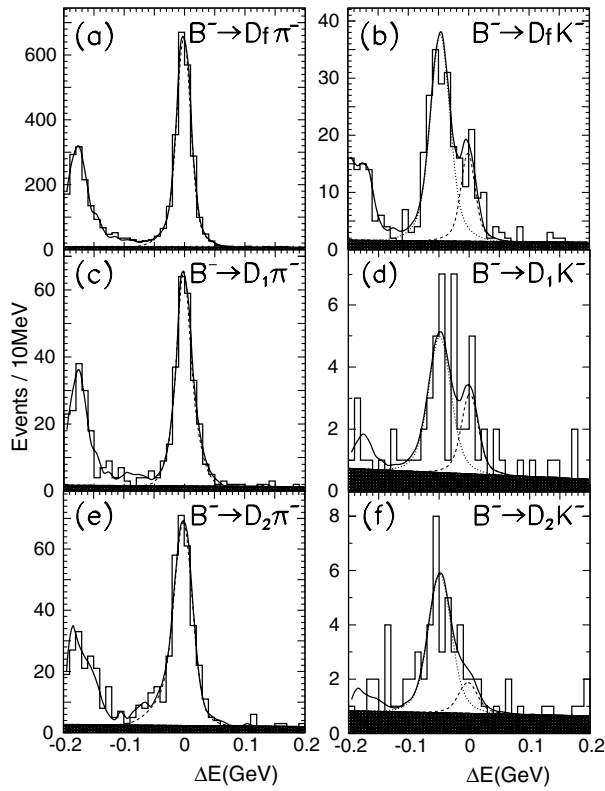


FIG. 1. ΔE distributions for $B^- \rightarrow D^0 \pi^- / K^-$ candidates and fit results: (a) $B^- \rightarrow D_f \pi^-$, (b) $B^- \rightarrow D_f K^-$, (c) $B^- \rightarrow D_1 \pi^-$, (d) $B^- \rightarrow D_1 K^-$, (e) $B^- \rightarrow D_2 \pi^-$, and (f) $B^- \rightarrow D_2 K^-$, where in each case the pion mass is assigned to the prompt π^- / K^- . Dotted (dashed) lines show the distributions of $DK(D\pi)$ signals. The shaded plot shows the continuum background and the remaining component from $B\bar{B}$ background is estimated and fitted by Monte Carlo simulation. In the DK plots, the dashed curves show the $D^0 \pi^-$ feed-across.

the ΔE distribution in the M_{lc} sideband region ($5.20 \text{ GeV}/c^2 < M_{lc} < 5.26 \text{ GeV}/c^2$). $B\bar{B}$ backgrounds, such as $B^- \rightarrow D^0 \rho^-$ and $B^- \rightarrow D^* \pi^-$ processes, are mostly seen at negative values of ΔE ; MC simulations are used to obtain the shape of their distribution.

TABLE I. Results of fits for the $D^0 \pi^-$ and $D^0 K^-$ decay modes. The event yields, the feed-across from $D^0 \pi^-$ to the $D^0 K^-$ signal region, statistical significance of $D^0 K^-$ signals, efficiencies, and branching fraction ratios (R) are given. Efficiencies are determined by weighting according to the measured subcomponents [$\eta \equiv \sum_i \eta_i \mathcal{B}(D^0 \rightarrow X_i)$]. The results with the dominant decay mode of $D_{1,2}$ are also shown in parentheses.

	$B^- \rightarrow D^0 K^-$ events	$B^- \rightarrow D^0 \pi^-$ feed-across	Stat. sig.	$B^- \rightarrow D^0 \pi^-$ events	Efficiency (%) $\eta(D^0 \pi^-) / \eta(D^0 K^-)$	Branching fraction ratio R
$B^- \rightarrow D_f h^-$	161.7 ± 14.5	51.3 ± 9.7	16.9	2245.1 ± 51.0	1.703/1.639	$0.094 \pm 0.009 \pm 0.007$
$B^- \rightarrow D_1 h^-$ ($D_1 \rightarrow K^- K^+$)	22.9 ± 6.1 (18.9 ± 5.2)	9.6 ± 4.4 (9.0 ± 3.7)	5.1	240.1 ± 16.7 (202.0 ± 14.8)	0.173/0.165 (0.142/0.136)	$0.125 \pm 0.036 \pm 0.010$ (0.122 ± 0.035)
$B^- \rightarrow D_2 h^-$ ($D_2 \rightarrow K_S \pi^0$)	26.1 ± 6.5 (14.8 ± 4.7)	4.9 ± 4.1 (1.0 ± 2.2)	5.5	290.6 ± 19.1 (171.5 ± 13.9)	0.184/0.173 (0.119/0.113)	$0.119 \pm 0.028 \pm 0.006$ (0.114 ± 0.037)

In the fits to the $B^- \rightarrow D^0 \pi^-$ enriched ΔE distribution, the signal peak position and width, and the normalization of continuum and $B\bar{B}$ backgrounds are free parameters. In the fits to the $B^- \rightarrow D^0 K^-$ enriched sample, we calibrate the shape parameters of the $B^- \rightarrow D^0 K^-$ double Gaussian using the $B^- \rightarrow D^0 \pi^-$ data, following the procedure described in [4]: the $B^- \rightarrow D^0 \pi^-$ distribution is fitted using a kaon mass hypothesis for the prompt pion, and the relative peak position is then reversed with respect to the origin. This accounts for the kinematical shifts and smearing of the ΔE peaks caused by the incorrect mass assignment. The shape parameters for the feed-across from $B^- \rightarrow D^0 \pi^-$ are fixed using the fit results of the $B^- \rightarrow D^0 \pi^-$ enriched sample.

The fit results are shown as solid curves in Fig. 1. The statistical significance of both $D_1 K^-$ and $D_2 K^-$ signals, defined as $\sqrt{-2 \ln(\mathcal{L}_0 / \mathcal{L}_{\max})}$, is over 5.0σ . (\mathcal{L}_{\max} is the maximum likelihood in the ΔE fit and \mathcal{L}_0 is the likelihood when the signal yield is constrained to be zero.) The results are summarized in Table I.

The ratio of branching fractions is determined using

$$R = \frac{N(B^- \rightarrow D^0 K^-)}{N(B^- \rightarrow D^0 \pi^-)} \times \frac{\eta(B^- \rightarrow D^0 \pi^-)}{\eta(B^- \rightarrow D^0 K^-)} \times \frac{\epsilon(\pi)}{\epsilon(K)}, \quad (2)$$

where N is the number of events obtained, η is the signal detection efficiency, and ϵ is the prompt hadron identification efficiency. The signal detection efficiencies are determined from MC simulation: $\eta(B^- \rightarrow D^0 K^-)$ is approximately 5% lower than $\eta(B^- \rightarrow D^0 \pi^-)$ due to kaon decays in flight. Particle identification efficiencies $\epsilon(K)$, $\epsilon(\pi)$ are determined from a kinematically selected sample of $D^{*+} \rightarrow D^0 \pi^+$, $D^0 \rightarrow K^- \pi^+$ decays, using tracks in the same c.m. momentum ($p^{\text{c.m.}}$) and polar angle regions as prompt hadrons from $B^- \rightarrow Dh^-$ decay ($2.1 \text{ GeV}/c < p^{\text{c.m.}} < 2.5 \text{ GeV}/c$). For $P(K/\pi) > 0.8$, we find $\epsilon(K) = 0.778 \pm 0.005$ with a pion misidentification rate of 0.024 ± 0.002 ; $P(K/\pi) < 0.8$ gives a pion identification efficiency $\epsilon(\pi) = 0.972 \pm 0.007$.

Since the kinematics of the $B^- \rightarrow D^0 K^-$ and $B^- \rightarrow D^0 \pi^-$ processes are similar, the systematic uncertainties from detection efficiencies cancel in the ratios of

TABLE II. Summary of measured partial rate asymmetries.

Mode	$N(B^+)$	$N(B^-)$	\mathcal{A}_{CP}	90% C.L.
$B^\pm \rightarrow D_f K^\pm$	80.6 ± 10.1	81.1 ± 10.4	$0.003 \pm 0.089 \pm 0.037$	$-0.15 < \mathcal{A}_f < 0.16$
$B^\pm \rightarrow D_1 K^\pm$	8.1 ± 3.9	14.7 ± 4.6	$0.29 \pm 0.26 \pm 0.05$	$-0.14 < \mathcal{A}_1 < 0.73$
$B^\pm \rightarrow D_2 K^\pm$	16.4 ± 5.5	10.6 ± 4.2	$-0.22 \pm 0.24 \pm 0.04$	$-0.62 < \mathcal{A}_2 < 0.18$

branching fractions. The dominant systematic errors are the uncertainties in the shapes of backgrounds in the ΔE distributions (5.1%–7.9%), which are determined by varying the background shape of the fitting function by $\pm 1\sigma$, and K/π identification efficiencies (1.2%). The sum of the uncertainties for each mode are combined in quadrature to determine the total systematic errors for the ratios.

The resulting measurements of R are listed with their statistical and systematic errors in Table I. These are the first observations of the decays $B^- \rightarrow D_{CP}K^-$. As a check, the result for the flavor specific decay $B^- \rightarrow D_f h^-$ is listed as well, and is found to be consistent with previous measurements. We find no deviation of the R ratio for the $B^- \rightarrow D_{CP}K^-$ processes from the corresponding flavor specific modes beyond statistical errors.

To search for direct CP violation, we measure the partial rate asymmetries $\mathcal{A}_{1,2}$ in $B^\pm \rightarrow D_{1,2}K^\pm$ decays, fitting the B^+ and B^- yields separately for each mode. The results are shown in Table II. To construct 90% confidence intervals in \mathcal{A} , we combine statistical and systematic errors in quadrature, and assume that the total error is distributed as a Gaussian. We find $-0.14 < \mathcal{A}_1 < 0.73$ and $-0.62 < \mathcal{A}_2 < 0.18$, consistent with zero asymmetry. We also measure \mathcal{A} for the flavor specific mode, and find a result consistent with zero, as expected.

The main sources of systematic errors for the partial rate asymmetries \mathcal{A} are possible asymmetries in the measured background (1.5% – 3.9%), intrinsic asymmetry in the Belle detector (3.6%), and kaon identification (1.0%). We observe 1154.6 ± 35.4 $B^+ \rightarrow \bar{D}^0 \pi^+$, $\bar{D}^0 \rightarrow K^+ \pi^-$, and 1073.5 ± 34.5 $B^- \rightarrow D^0 \pi^-$, $D^0 \rightarrow K^- \pi^+$ candidates, consistent with our expectation that the detector has no significant intrinsic charge asymmetry. Using MC simulation, we find that the contribution of nonresonant contaminations ($\sim 0.1\%$) of ω and ϕ can be neglected.

In conclusion, using 29.1 fb^{-1} of data collected with the Belle detector, we report studies of the decays $B^\pm \rightarrow D_{CP}K^\pm$. The ratios of branching fractions R for the decays $B^- \rightarrow D_{CP}K^-$ and $B^- \rightarrow D_{CP}\pi^-$ are consistent with that for the flavor specific decay within errors. The partial rate asymmetries $\mathcal{A}_{1,2}$ are consistent with zero within large errors. This is the first stage of a program to measure the angle ϕ_3 in the CKM unitarity triangle.

We wish to thank the KEKB accelerator group for the excellent operation of the KEKB accelerator. We acknowledge support from the Ministry of Education, Culture, Sports, Science, and Technology of Japan and the Japan Society for the Promotion of Science; the Australian Research Council and the Australian Department of Industry, Science and Resources; the National Science Foundation of China under Contract No. 10175071; the Department of Science and Technology of India; the BK21 program of the Ministry of Education of Korea and the CHEP SRC program of the Korea Science and Engineering Foundation; the Polish State Committee for Scientific Research under Contract No. 2P03B 17017; the Ministry of Science and Technology of the Russian Federation; the Ministry of Education, Science and Sport of the Republic of Slovenia; the National Science Council and the Ministry of Education of Taiwan; and the U.S. Department of Energy.

*On leave from Nova Gorica Polytechnic, Nova Gorica.

- [1] M. Gronau and D. Wyler, Phys. Lett. B **265**, 172 (1991).
- [2] I. Dunietz, Phys. Lett. B **270**, 75 (1991); D. Atwood, I. Dunietz and A. Soni, Phys. Rev. Lett. **78**, 3257 (1997).
- [3] H. Quinn and A. I. Sanda, Eur. Phys. J. C **15**, 626 (2000).
- [4] Belle Collaboration, K. Abe *et al.*, Phys. Rev. Lett. **87**, 111801 (2001).
- [5] CLEO Collaboration, M. Athanas *et al.*, Phys. Rev. Lett. **80**, 5493 (1998).
- [6] Belle Collaboration, A. Abashian *et al.*, Nucl. Instrum. Methods Phys. Res., Sect. A **479**, 117 (2002).
- [7] KEKB accelerator group, *KEKB B-factory Design Report*, KEK Report No. 95-7, 1995 (unpublished).
- [8] For ω , θ_{hel} is the angle between the normal to the ω decay plane and the D momentum, as measured in the ω rest frame. For ϕ , θ_{hel} is the angle between the momenta of the parent D and daughter K mesons in the ϕ rest frame.
- [9] Belle Collaboration, K. Abe *et al.*, Phys. Rev. Lett. **87**, 101801 (2001). The index *so(oo)* indicates that the moment is calculated from pairs of particles where only one (neither) particle comes from the B candidate.
- [10] We use the QQ B -meson decay event generator developed by the CLEO Collaboration (<http://www.lns.cornell.edu/public/CLEO/soft/QQ>) and GEANT3 for the detector simulation; CERN Program Library Long Writeup No. W5013, CERN, 1993.